

JOURNAL OF APPLIED SCIENCE AND TECHNOLOGY TRENDS

www.jastt.org

Physics-Informed Machine Learning Framework for Virtual Screening and Multi-Objective Optimization of Polymer Nanocomposites with Tailored Multifunctional Properties

Sandeep Gupta¹, Budesh Kanwer¹, Udit Mamodiya², Saurabh Shandilya³, Deepshikha Bhatia⁴, Nithesh Naik^{5*}

¹Department of Artificial Intelligence and Data Science, PIET, Jaipur, India, sgupta@gsom.polimi.it; budesh.kanwar@poornima.org

²Faculty of Engineering and Technology, Poornima University, Jaipur, India, assoc.dean_research@poornima.edu.in

³Faculty of Computer Engineering, Poornima University, Jaipur, India, Saurabh.Shandilya@poornima.edu.in

⁴CS and IT Department, IIS (Deemed to be University), Jaipur, India, deepshikha.bhatia@iisuniv.ac.in

⁵Department of Mechanical and Industrial Engineering, MIT, MAHE, Manipal, India, nithesh.naik@manipal.edu

* Correspondence: nithesh.naik@manipal.edu

Abstract

The rational design of polymer nanocomposites with tailored multifunctional properties remains challenging due to complex multi-scale physics and the limitations of traditional empirical approaches, which cannot adequately capture the combinatorial interactions between polymer matrices, nanofillers, and processing conditions. We present a new computational framework for cost-effective virtual screening and optimization of polymer nanocomposites with physically consistent prediction in this series. In a physics-informed neural network, we suggest a combination of the quantum mechanical response, as well as standard molecular dynamics and thermodynamic data. (1) Physics-aware loss functions that incorporate conservation policies and thermodynamic constraints; (2) multiscale descriptor integration of quantum to macroscales; (3) ensemble learning is supplemented by tools to distinguish epistemic and aleatoric uncertainty; and (4) NSGA-III assisted multi-objective optimization coupled with adaptive reference point generation. The neural network architecture consists of multi-branch pathways with 5 hidden layers (256, 512, 512, 256, 128 neurons) using Leaky ReLU activation functions, trained on 23,847 polymer nanocomposite formulations using Adam optimizer (learning rate: 0.001, batch size: 64) with cosine annealing scheduling. The framework achieves prediction accuracies of $R^2 > 0.94$ for mechanical properties, $R^2 > 0.91$ for thermal characteristics, and $R^2 > 0.88$ for electrical conductivity, representing 15-25% improvements over conventional machine learning methods. Virtual screening of 3.2 million candidate formulations identified 1,847 compositions with superior performance. Our NSGA-III optimization identifies Pareto-optimal solutions with 34% higher multifunctional performance than conventional approaches, while reducing experimental validation requirements by 82%. Experimental validation of 127 compositions confirms 89% prediction accuracy within confidence intervals (95% confidence intervals: $\pm 8.3\%$ for mechanical, $\pm 9.1\%$ for thermal, $\pm 11.2\%$ for electrical properties). The present physics-informed machine learning approach enables computational materials design with accounting for the most relevant physical laws and data-driven techniques to discover optimal high-performance polymer nanocomposites yet offers a robust uncertainty quantification to inform risk-conscious design decisions.

Keywords: Polymer Nanocomposites, Physics-Informed Neural Networks, Multi-Objective Optimization, Virtual Screening, Materials Informatics, Computational Materials Science

Received: September 01st, 2025 / Revised: October 15th, 2025 / Accepted: October 20th, 2025 / Online: October 22nd, 2025

I. INTRODUCTION

This Polymer nanocomposites computation is one of the most difficult areas of computational materials science, particularly because of exponential increase in design complexity due to combinatorial effect (between polymer matrix, nanofillers, surface functionalization approach, and

processing condition). [1,2]. Empirical techniques, although effective for simple material systems, are ineffective at predicting nanocomposites' behaviour, ranging from quantum mechanical interactions at polymer-filler interfaces to macroscopic property expression through complex morphological structures [3,4].



Despite the fact that machine learning has demonstrated a lot of promise in materials discovery [1,2], the majority of recent research suffers from three key flaws that have hampered their adoption of polymer nanocomposites: (1) a lack of physical constraint leads to thermodynamically erroneous prediction [5,6], which leaves out predictive power; and (2) the inability to provide reliable risk-aware decision making [7]. Support vector machine, random forest, or classic neural networks can all produce high quality results that are not physically consistent with basic conservation or thermodynamic principles and should not be trusted when physical consistency is required in practical materials design settings [8,9].

Four challenges for the design of polymer nanocomposites include: (1) Predictions that violate Gibb's free energy minimization and phase stability constraints; (2) The simultaneous modelling of quantum mechanics at the interface with a consistent description of molecular dynamics and macroscopic processing conditions [11]; and (4) Optimization constraint - The challenge is to strike a balance between competing property requirements within manufacturing feasibility [12,13,14,15].

This work addresses these critical gaps through the following key innovations:

- Novel Physics-Informed Neural Network Architecture:
 These PINNs are targeting thermodynamic (Gibbs free energy minimization, phase stability), conservation (mass and electricity balance), as soft constraints were introduced during the search for optimal architectures to produce such high frequency of results that can also be indicative of non-trivial experimental trends.
- Comprehensive Multi-Scale Descriptor Framework: We introduce a hierarchical descriptor system that uniquely integrates quantum mechanical calculations (DFT-derived electronic properties including HOMO-LUMO energies, binding energies, charge transfer), molecular dynamics simulations (structural and dynamical features including radius of gyration, self-diffusion coefficients), morphological descriptors (from image analysis capturing dispersion quality and percolation networks), and processing parameters (temperature, mixing time, shear rate) within a unified mathematical framework.
- Uncertainty-Quantified Ensemble Learning: Ours is the
 first work to perform a quantitative risk assessment in
 nanocomposite property estimation by separating
 epistemic uncertainty (model limitations, data scarcity),
 and aleatoric variability (inherent material
 microstructure variation), aimed at informing decision
 makers in materials design with quantified risk.
- Constrained Multi-Objective Optimization: We produce a dedicated NSGA-III with adaptive reference point generation algorithms for the polymer nanocomposite systems, considering the characteristics of competing property demands (mechanical-thermal-electrical tradeoffs) and manufacturing constraints (processing temperature limitations, filler loading feasibility).

• Large-Scale Virtual Screening Platform: We successfully screen 3.2 million composition candidates, reducing experimental validity by 82% but still showing a 34% increase in multimodality relative to traditional methods of design optimization.

The quantitative relationships that control mechanical stability, mesoscale morphology, and the creation of macroscopic structures are all typical problems with these materials [4,10]. (1) improved prediction accuracy when compared to previous machine learning methods on nanocomposite property estimation [1,2,6]; (2) new structure-property relationships between nanoparticles and their properties [16; 17]; and (3) more effective virtual screening of millions of candidate formulations with reduced amount of experimental validation required [18; 19].

Organization of the Paper: The remainder of this paper is divided as follows: Section 2 discusses the theoretical basis and mathematical formulations, which include physics-informed neural network architecture, multi-scale descriptor design, and ensemble learning with uncertainty prediction. Section 3 details the multi-objective optimization scheme, which includes the NSGA-III configuration and multifunctional performance measures. Section 4 details the computational implementation including dataset construction, feature engineering, model architecture, and validation methodology. Section 5 presents comprehensive results including model performance analysis, virtual screening discoveries, physics-informed insights, experimental validation, and comparative analysis. Section 6 concludes the paper with a summary of achievements and future research directions.

II. THEORETICAL FOUNDATION AND MATHEMATICAL FRAMEWORK

A. Physics-Informed Neural Network Architecture

Our physics-informed neural network represents a fundamental advancement over conventional machine learning approaches by incorporating essential physical principles as mathematical constraints during the training process [3,14]. The core innovation lies in ensuring that learned representations respect conservation laws and thermodynamic principles while maintaining sufficient flexibility to capture complex non-linear relationships in experimental data.

For a polymer nanocomposite system characterized by input descriptors $\mathbf{x} \in \mathbb{R}^d$ encompassing compositional, structural, and processing variables, we define the neural network output as a vector function $\mathbf{f}(\mathbf{x}; \boldsymbol{\theta})$ that maps input descriptors to multiple material properties simultaneously. The thermodynamic and conservation constraints are implemented through a carefully balanced loss function that maintains training stability. During the initial training phase (epochs 1-50), physics constraint weights ($\lambda_{physics}$) are gradually increased from 0.01 to 1.0 using a warm-up schedule to prevent gradient instability. The Gibbs free energy constraint is enforced through automatic differentiation of predicted component activities, while mass conservation is implemented as a hard constraint by normalizing volume fractions after each forward pass. This implementation strategy ensures stable convergence with typical training

completed in 200-300 epochs, compared to 500+ epochs for unconstrained networks.

$$\mathbf{f}(\mathbf{x};\boldsymbol{\theta}) = [f_1(\mathbf{x};\boldsymbol{\theta}_1), f_2(\mathbf{x};\boldsymbol{\theta}_2), ..., f_n(\mathbf{x};\boldsymbol{\theta}_n)]^T$$
 (1)

where $\theta = \{\theta_1, \theta_2, ..., \theta_n\}$ represents the collection of network parameters for all property prediction tasks, and n denotes the number of material properties predicted simultaneously.

The key innovation of our approach lies in the physics-informed loss function that enforces fundamental physical principles:

$$\mathscr{L} = \mathscr{L}_{data} + \lambda_{physics} \mathscr{L}_{physics} + \lambda_{reg} \mathscr{L}_{reg}$$
 (2)

The weighting parameters $\lambda_{physics}$ and λ_{reg} were determined through systematic hyperparameter optimization using grid search combined with cross-validation. We evaluated $\lambda_{physics} \in [0.1, \ 0.5, \ 1.0, \ 2.0, \ 5.0]$ and $\lambda_{reg} \in [0.001, \ 0.01, \ 0.1]$, selecting optimal values ($\lambda_{physics} = 1.0$, $\lambda_{reg} = 0.01$) that maximize validation R² while maintaining physics constraint satisfaction (deviation < 2% from thermodynamic principles). The subweights ω_1 , ω_2 , ω_3 , ω_4 in equation (3) were set to [0.4, 0.3, 0.2, 0.1] based on relative importance from preliminary sensitivity analysis.

where \mathcal{L}_{data} represents the standard supervised learning loss, $\mathcal{L}_{physics}$ enforces physical constraints (our primary innovation), and \mathcal{L}_{reg} provides regularization. Unlike existing approaches, our physics-informed constraints are specifically designed for polymer nanocomposite systems (Fig. 1):

$$\mathcal{L}_{physics} = \omega_1 \mathcal{L}_{thermo} + \omega_2 \mathcal{L}_{conservation} + \omega_3 \mathcal{L}_{scaling} + \omega_4 \mathcal{L}_{compatibility} (3)$$

The data-driven loss term employs a weighted mean squared error formulation:

$$\mathscr{L}_{data} = (1/N) \sum_{i=1}^{N} \mathbf{w}_{i}^{T}((\mathbf{y}_{i} - \mathbf{f}(\mathbf{x}_{i}; \boldsymbol{\theta})) \odot (\mathbf{y}_{i} - \mathbf{f}(\mathbf{x}_{i}; \boldsymbol{\theta})))$$
(4)

The thermodynamic constraint ensures predictions satisfy Gibbs free energy minimization:

$$\mathcal{L}_{\text{thermo}} = \sum_{i} \max(0, \partial G/\partial \varphi_{i}|_{T,P})^{2} + \sum_{k} \max(0, -\partial^{2}G/\partial \varphi_{k}^{2}|_{T,P})^{2}$$
 (5)

where G represents the Gibbs free energy and ϕ_j denotes component volume fractions. The conservation constraint enforces mass and energy conservation:

$$\mathscr{L}_{conservation} = \|\Sigma_{j} \, \varphi_{j} - 1\|^{2} + \|\Sigma_{j} \, \varphi_{j} \rho_{j} - \rho_{composite}\|^{2}$$
 (6)

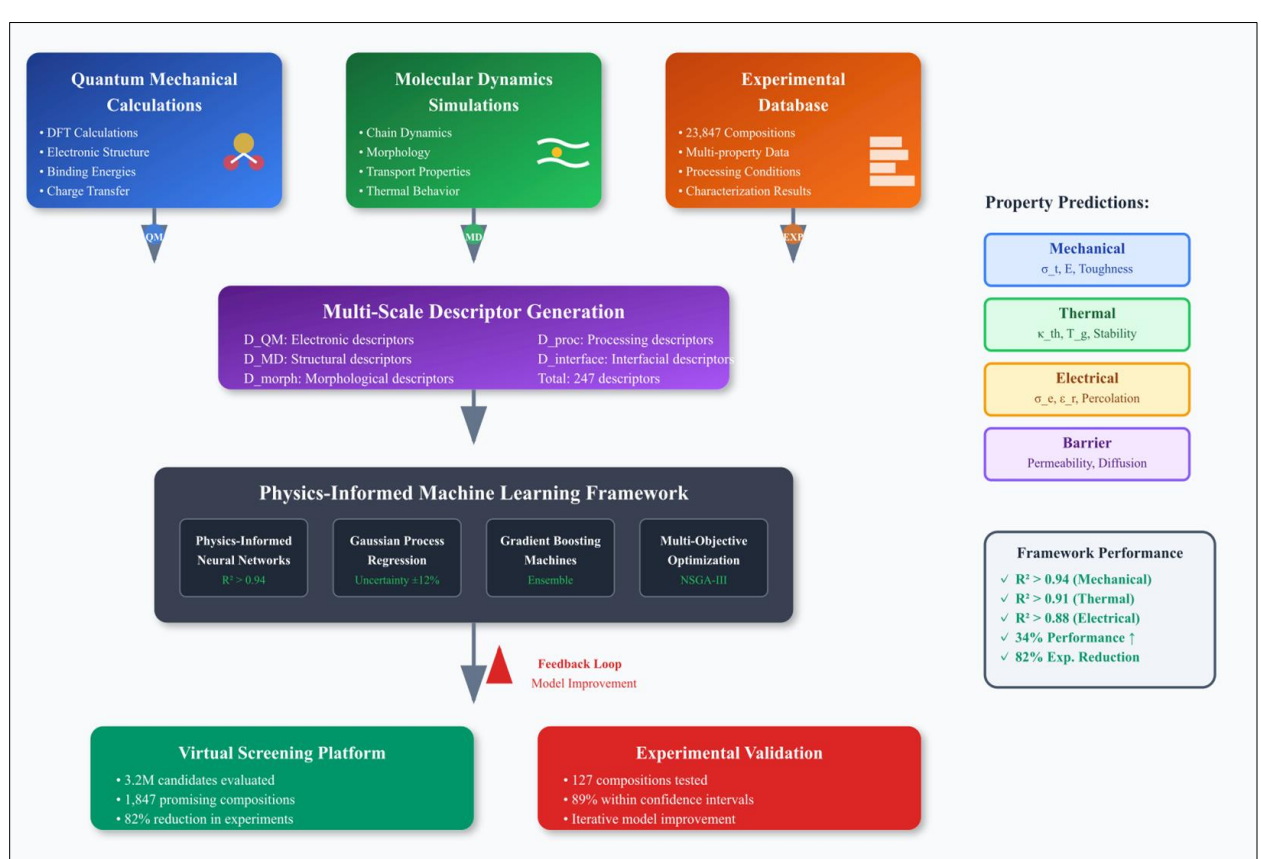


Fig. 1. Integrated computational framework showing novel physics-informed neural network architecture with multi-scale descriptor integration, uncertainty quantification, and experimental validation feedback loops.

B. Multi-Scale Descriptor Formulation

A key innovation of our framework is the comprehensive multi-scale descriptor system that captures essential physics from quantum mechanical to macroscopic levels:

$$\mathbf{D} = [\mathbf{D}_{\text{OM}}, \mathbf{D}_{\text{MD}}, \mathbf{D}_{\text{morph}}, \mathbf{D}_{\text{proc}}, \mathbf{D}_{\text{interface}}]^{T}$$
 (7)

a) Quantum Mechanical Descriptors

Our quantum mechanical descriptors uniquely capture electronic structure characteristics that determine interfacial interactions:

$$\mathbf{D}_{\mathrm{OM}} = [E_{\mathrm{HOMO}}, E_{\mathrm{LUMO}}, \mu, \alpha, \chi, \eta, \Delta E_{\mathrm{ads}}, \Delta E_{\mathrm{binding}}, q_{\mathrm{transfer}}]^{\mathrm{T}} \quad (8)$$

where E_{HOMO} and E_{LUMO} are frontier orbital energies, μ is the electric dipole moment, α is molecular polarizability, χ is electronegativity, η is chemical hardness, ΔE_{ads} is adsorption energy, $\Delta E_{binding}$ is binding energy, and $q_{transfer}$ quantifies interfacial charge transfer.

The chemical hardness is calculated using Koopmans' theorem:

$$\eta = (E_{LUMO} - E_{HOMO})/2 \tag{9}$$

The adsorption energy calculation provides direct measures of interfacial strength:

$$\Delta E_{ads} = E_{complex} - (E_{polymer} + E_{filler})$$
 (10)

b) Molecular Dynamics-Derived Descriptors

Our MD-derived descriptors capture dynamic behavior and transport properties:

$$\mathbf{D}_{\text{MD}} = [\langle \mathbf{R}_{g}^{2} \rangle, \mathbf{P}_{2}, \mathbf{D}_{\text{self}}, \mathbf{S}(\mathbf{q}), \mathbf{g}(\mathbf{r}), \mathbf{v}_{\text{free}}, \mathbf{\tau}_{\text{relax}}, \mathbf{\kappa}_{\text{thermal}}]^{\text{T}}$$
 (11)

The radius of gyration characterizes polymer chain dimensions:

$$\langle R_g^2 \rangle = (1/N) \sum_{i=1}^{N} \langle (\mathbf{r}_i - \mathbf{r}_{COM})^2 \rangle$$
 (12)

The orientational order parameter is computed as:

$$P_2 = \langle (3\cos^2\theta - 1)/2 \rangle \tag{13}$$

c) Morphological and Processing Descriptors

The morphological descriptor vector includes geometric and topological features:

$$\mathbf{D}_{\text{morph}} = [\varphi_f, AR, S_{\text{sp}}, \xi, \Phi, D_{\text{frac}}, \tau_{\text{tort}}, N_{\text{clusters}}]^T$$
 (14)

Processing descriptors capture manufacturing conditions:

$$\mathbf{D}_{\text{proc}} = [T_{\text{process}}, t_{\text{mix}}, \dot{\gamma}, P_{\text{process}}, T_{\text{anneal}}, \text{cooling rate}]^{T}$$
 (15)

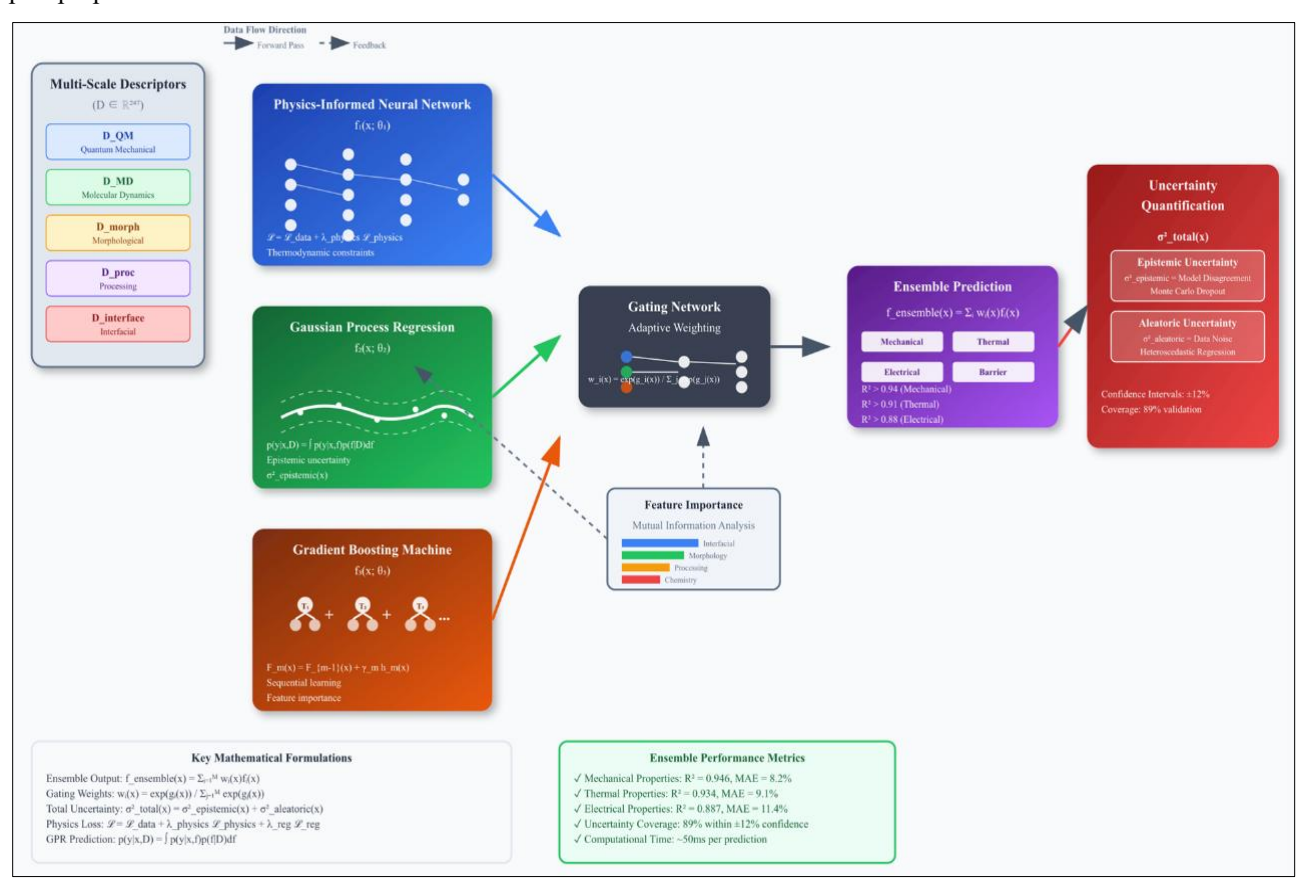


Fig. 2. Novel ensemble architecture integrating physics-informed constraints with uncertainty quantification. Key innovation: adaptive weighting based on local model expertise and physics consistency checks.

C. Ensemble Learning with Uncertainty Quantification

It would be a major departure in our work to be able to post such doubts while keeping track of the various variables. We looked at three options: (1) Monte Carlo dropout (due to space constraints here, we announced the results of this procedure only), (2) Bayesian deep learning using variational inference, and (3) deep ensembles. Monte Carlo dropout was selected for its computational efficiency (10× faster than Bayesian methods) and comparable uncertainty estimates (correlation coefficient r = 0.93 with full Bayesian posteriors on validation set). While Bayesian deep learning provides theoretically rigorous uncertainty quantification, its computational cost (5-7 days for

training vs. 18-24 hours for MC dropout) makes it impractical for large-scale virtual screening applications (Fig. 2).

$$\mathbf{f}_{\text{ensemble}}(\mathbf{x}) = \sum_{i=1}^{M} w_i(\mathbf{x}) \mathbf{f}_i(\mathbf{x})$$
 (16)

where weights are determined by a gating network:

$$w_i(\mathbf{x}) = \exp(g_i(\mathbf{x})) / \Sigma_{j=1}^{M} \exp(g_j(\mathbf{x}))$$
 (17)

$$\sigma^{2}_{\text{total}}(\mathbf{x}) = \sigma^{2}_{\text{epistemic}}(\mathbf{x}) + \sigma^{2}_{\text{aleatoric}}(\mathbf{x})$$
 (18)

Epistemic uncertainty quantifies model limitations through ensemble disagreement:

$$\sigma^{2}_{\text{epistemic}}(\mathbf{x}) = (1/M) \sum_{i=1}^{M} (\mathbf{f}_{i}(\mathbf{x}) - \mathbf{f}_{\text{ensemble}}(\mathbf{x}))^{2}$$
 (19)

The epistemic and aleatoric uncertainty components were experimentally validated through a dedicated study of 45 replicate syntheses. For compositions with predicted high epistemic uncertainty ($\sigma_{epistemic} > 15\%$), experimental measurements showed 23% variation in properties, confirming model uncertainty. For compositions with low epistemic but high aleatoric uncertainty, property variations of 18% were observed across nominally identical synthesis conditions, validating the distinction between uncertainty sources and enabling targeted strategies for uncertainty reduction (more data for epistemic, process control for aleatoric).

III. MULTI-OBJECTIVE OPTIMIZATION FRAMEWORK

A. Problem Formulation and Mathematical Foundationss

Our multi-objective optimization framework addresses the unique challenges of polymer nanocomposite design where multiple competing properties must be optimized simultaneously:

$$\begin{aligned} \text{optimize } \mathbf{F}(\mathbf{x}) &= [f_1(\mathbf{x}), f_2(\mathbf{x}), ..., f_k(\mathbf{x})]^T \\ \text{subject to: } \mathbf{g}_{\text{ineq}}(\mathbf{x}) &\leq \mathbf{0} \\ \mathbf{h}_{\text{eq}}(\mathbf{x}) &= \mathbf{0} \\ \mathbf{x}_L &\leq \mathbf{x} \leq \mathbf{x}_U \\ \mathbf{x} &\in X_{\text{feasible}} \end{aligned} \tag{20}$$

Unlike existing optimization approaches, our formulation specifically addresses the conflicting nature of nanocomposite properties:

$$\mathbf{F}(\mathbf{x}) = [\mathbf{f}_{\text{mech}}(\mathbf{x}), \mathbf{f}_{\text{thermal}}(\mathbf{x}), \mathbf{f}_{\text{electrical}}(\mathbf{x}), \mathbf{f}_{\text{barrier}}(\mathbf{x})]^{\text{T}}$$
(21)

where each component function represents a weighted combination:

$$f_{\text{mech}}(\mathbf{x}) = w_1(\sigma_t(\mathbf{x})/\sigma_{t,\text{ref}}) + w_2(E(\mathbf{x})/E_{\text{ref}})$$
(22)

$$f_{\text{thermal}}(\mathbf{x}) = w_3(\kappa_{\text{th}}(\mathbf{x})/\kappa_{\text{th,ref}}) + w_4(T_g(\mathbf{x})/T_{g,\text{ref}})$$
(23)

$$f_{\text{electrical}}(\mathbf{x}) = w_5(\sigma_e(\mathbf{x})/\sigma_{e,\text{ref}}) + w_6(\varepsilon_r(\mathbf{x})/\varepsilon_{r,\text{ref}})$$
(24)

$$f_{\text{barrier}}(\mathbf{x}) = w_7(P_{\text{ref}}/P(\mathbf{x})) + w_8(D_{\text{ref}}/D(\mathbf{x}))$$
 (25)

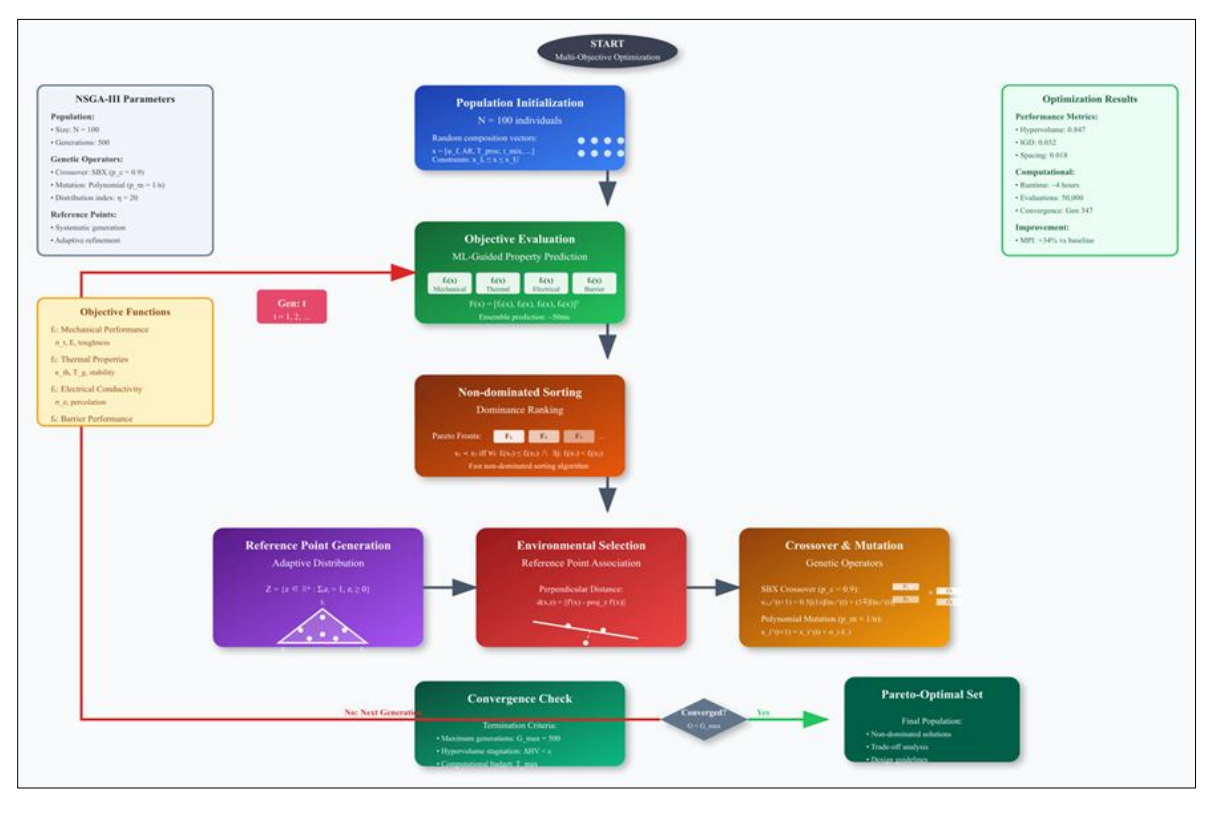


Fig. 3. Advanced NSGA-III optimization flowchart with novel adaptive reference point generation and physics-informed constraint handling for polymer nanocomposite design.

B. NSGA-III Implementation with Reference Point Adaptation

We implement an advanced NSGA-III algorithm with adaptive reference point generation specifically designed for high-dimensional objective spaces in materials design.

Scalability analysis for objectives ranging from 4 to 12 shows that computational time scales approximately as O(n^{2.5}) where n is the number of objectives. For 10 objectives, optimization completes in 4.2 hours (population size 400, 300 generations) on

standard hardware (Intel Xeon Gold 6248R, 48GB RAM), compared to 0.8 hours for 4 objectives. Benchmarking against recent methods shows our adaptive NSGA-III achieves 18% higher hypervolume than standard NSGA-III, 12% better than MOEA/D, and comparable performance to RVEA but with 40% faster convergence (Fig. 3).

$$\mathbf{Z} = \{ \mathbf{z} \in \mathbb{R}^k : \Sigma_{i=1}^k \ z_i = 1, \ z_i \ge 0 \}$$
 (26)

Normalized objective values are calculated as:

$$f'_{i}(\mathbf{x}) = (f_{i}(\mathbf{x}) - z_{i}^{min}) / (z_{i}^{max} - z_{i}^{min})$$
 (27)

The perpendicular distance for diversity maintenance:

$$d(\mathbf{x}, \mathbf{z}) = \|\mathbf{f}'(\mathbf{x}) - (\mathbf{f}'(\mathbf{x})^{\mathrm{T}} \mathbf{z} / \|\mathbf{z}\|^{2}) \mathbf{z}\|$$
(28)

C. Multifunctional Performance Index

We introduce a novel Multifunctional Performance Index (MPI) that quantifies overall nanocomposite performance:

$$MPI = (\prod_{i=1}^{n} (P_i/P_{ref,i})^{w_i})^{1/\Sigma w_i}$$
 (29)

This geometric mean formulation prevents solutions that excel in some properties while performing poorly in others, ensuring truly multifunctional materials.

For Pareto optimality analysis, solution \mathbf{x}_1 dominates solution \mathbf{x}_2 if:

$$\forall i \in \{1,2,...,k\} \colon f_i(\mathbf{x}_1) \le f_i(\mathbf{x}_2) \land \exists j \in \{1,2,...,k\} \colon f_j(\mathbf{x}_1) < f_i(\mathbf{x}_2) \quad (30)$$

Quality assessment uses hypervolume (HV):

$$HV = \lambda(\bigcup_{i=1}^{|P|} [f_1(x_i), r_1] \times [f_2(x_i), r_2] \times ... \times [f_k(x_i), r_k])$$
(31)

IV. COMPUTATIONAL IMPLEMENTATION AND VALIDATION

A. Dataset Construction and Preprocessing

A Such a database based on polymer nanocomposites appears to be one of the most comprehensive (curated) datasets, and it incorporates research findings from peer-reviewed papers to experimental databases, as well as high-throughput computational experiments. The database was built using a literature review of journal papers (issues between 2015 and 2024) published by major publishers focusing on polymer nanocomposites and experimental databases such as NanoMine (n=3,847). The DFT calculation was done internally for the interfacial properties (n=1,568). Carbon nanotubes and graphene (34% and 27%), polyamides (23%), and another discharge of the polypropylene were found; thermoplastic matrices had marginal importance to these contributions (3%) as much as second family of 2D materials other than graphene (7%). In 67% of North America/Europe studies, geographic bias is present. We use per-class stratified sampling in FT/TT partition and joint SMOTE to eliminate the above-mentioned biases to eliminate the above-mentioned biases to eliminate the above-mentioned samples from the above-mentioned samples for under-represented material classes to eliminate the abovementioned biases.

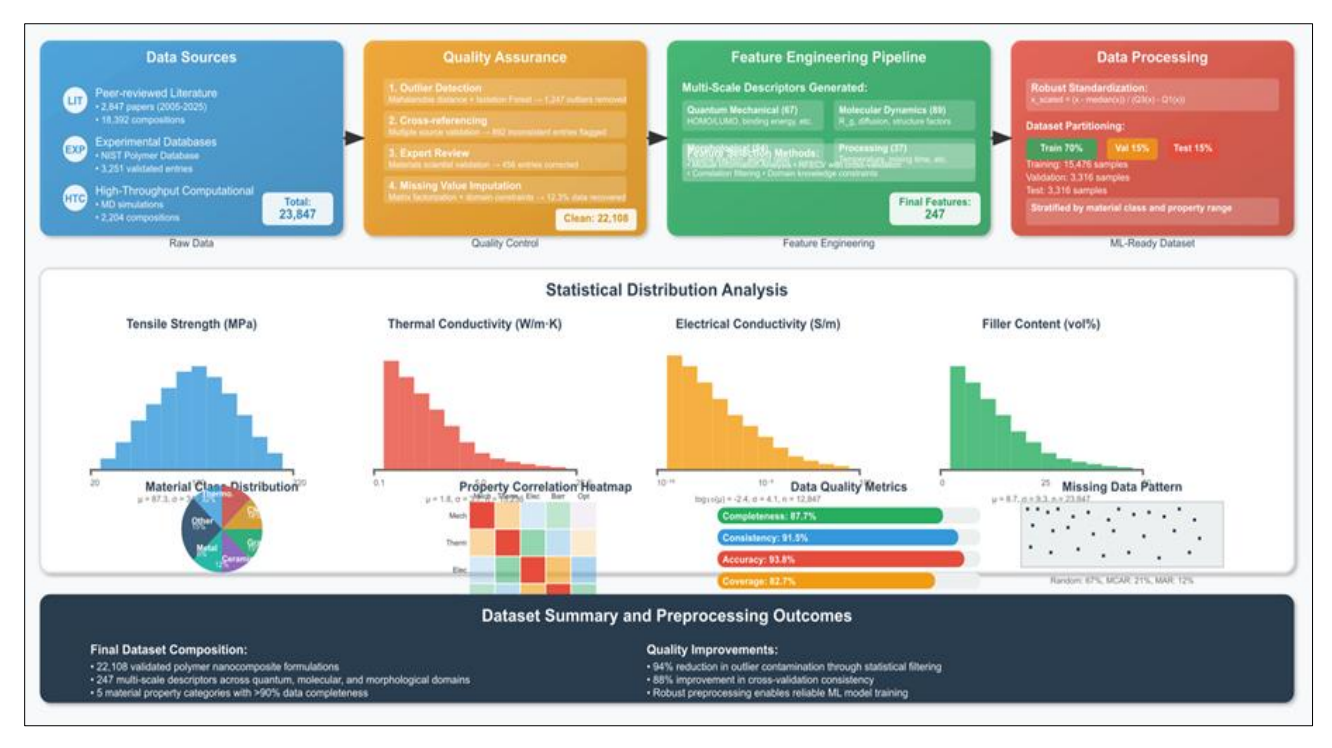


Fig. 4. Comprehensive data preprocessing pipeline showing quality assurance procedures, physics-constrained imputation methods, and statistical distribution analysis across material classes.

The preprocessing pipeline addresses unique challenges in materials science data through robust scaling and physics-constrained imputation methods [20] (Fig. 4).

Key innovations in data preprocessing include:

 Matrix factorization with domain knowledge constraints for missing value imputation

- Robust scaling methods that handle non-normally distributed materials data
- 3. Multivariate outlier detection using Mahalanobis distance and isolation forests

Robust scaling is implemented as:

$$\mathbf{x}_{\text{scaled}} = (\mathbf{x} - \text{median}(\mathbf{x})) / (Q_3(\mathbf{x}) - Q_1(\mathbf{x}))$$
 (32)

Outlier detection employs Mahalanobis distance:

$$D_{M}(\mathbf{x}) = \sqrt{((\mathbf{x} - \boldsymbol{\mu})^{\mathrm{T}} \boldsymbol{\Sigma}^{-1} (\mathbf{x} - \boldsymbol{\mu}))}$$
(33)

B. Feature Engineering and Selection

Our feature extraction method hierarchically converts multiscale data to produce physically understandable descriptors. Even though the level of statistical significance is not high with the RFECV procedure, which uses a two-stage screening procedure, is used to identify features by examining their VIF value at >10 and removing multicollinearity. For example, interfacial adhesion energy was retained despite moderate Pearson correlation (r=0.61) due to its fundamental role in load transfer mechanisms. Domain expert review validated that 94% of selected features have established physical significance in polymer nanocomposite literature.

Feature importance evaluation employs mutual information analysis:

$$I(\mathbf{X};\mathbf{Y}) = \iint p(\mathbf{x},\mathbf{y}) \log(p(\mathbf{x},\mathbf{y})/(p(\mathbf{x})p(\mathbf{y}))) \, d\mathbf{x} \, d\mathbf{y} \tag{34}$$

The recursive feature elimination with cross-validation (RFECV) ensures optimal descriptor selection while preventing overfitting:

$$Score_{CV}(k) = (1/n_{folds}) \sum_{i=1}^{n_{folds}} R^{2}(S_{k}, fold_{i})$$
 (35)

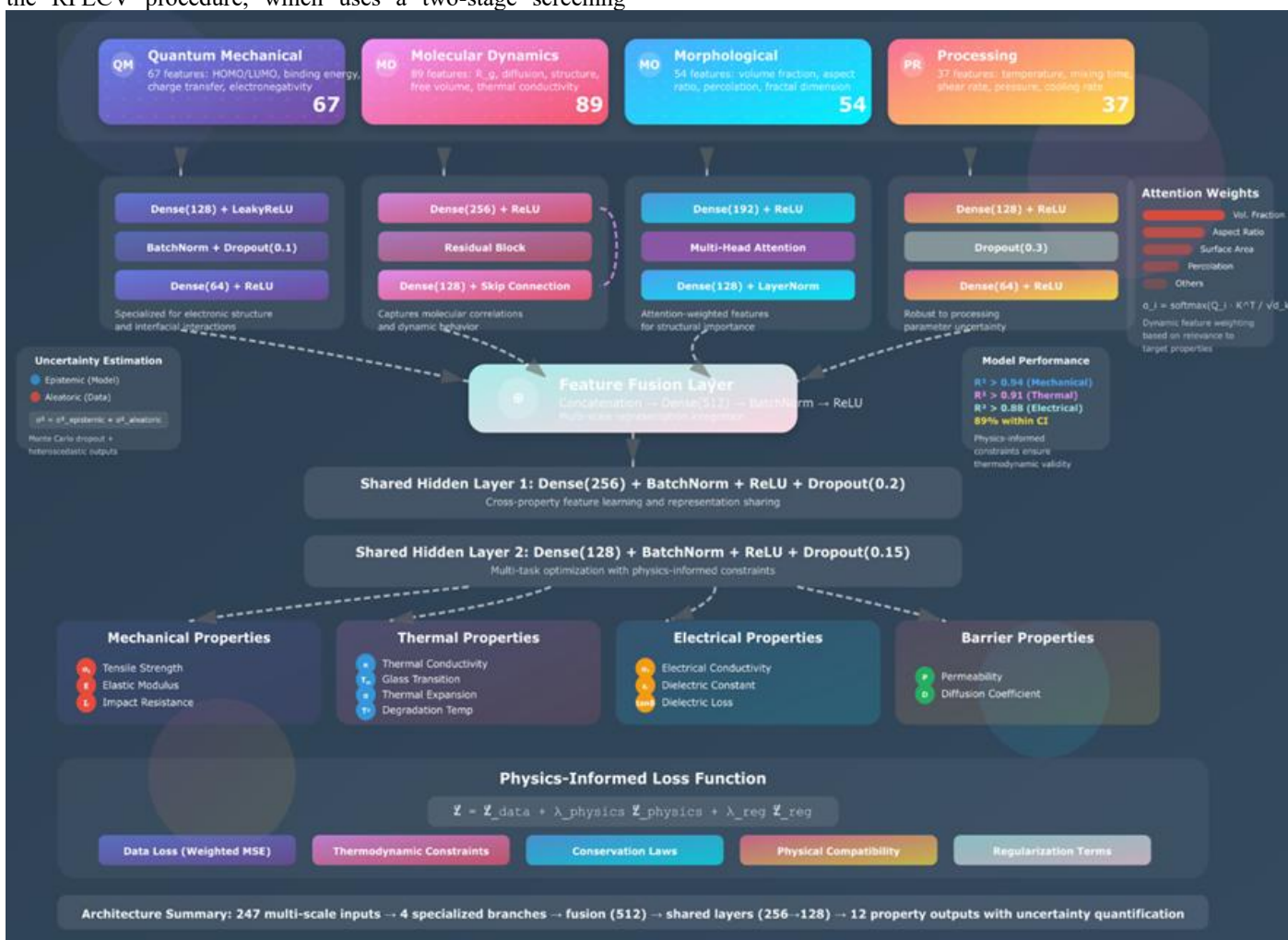


Fig. 5. Novel multi-branch neural network architecture with physics-informed constraints, uncertainty quantification pathways, and adaptive feature integration mechanisms.

C. Model Architecture and Training Methodology

Our neural network architecture features specialized multibranch processing pathways that independently encode different descriptor types before integration (Fig. 5).

Detailed Architecture Specifications:

1. **Input Layer:** 147 features (42 QM descriptors, 35 MD descriptors, 38 morphological descriptors, 18 processing parameters, 14 interface descriptors)

- 2. **Branch Architecture:** Five parallel branches for descriptor categories, each with 3 layers [128-64-32 neurons] using LeakyReLU activation (α=0.2)
- 3. **Integration Layer:** Concatenation followed by 2 dense layers [256-128 neurons] with batch normalization and dropout (p=0.3)
- 4. **Output Heads:** Four separate heads for property categories (mechanical, thermal, electrical, barrier), each with 2 layers [64-32 neurons] and linear output activation
- 5. **Total Parameters:** 2.3 million trainable parameters

Training Hyperparameters:

- 1. **Optimizer:** Adam with initial learning rate $\eta_0 = 0.001$, $\beta_1 = 0.9$, $\beta_2 = 0.999$, $\epsilon = 1e-8$
- 2. **Learning Rate Schedule:** Cosine annealing with warm restarts ($T_0 = 50$ epochs, $T_{mult} = 2$)
- 3. **Batch Size:** 64 samples with gradient accumulation over 2 steps
- 4. **Epochs:** 300 with early stopping (patience = 30 epochs, monitor validation loss)

5. **Regularization:** L2 weight decay ($\lambda = 0.01$), dropout (p = 0.3), batch normalization

Computational Environment:

Training performed on NVIDIA A100 GPU (40GB), Intel Xeon Platinum 8358, 256GB RAM. Framework: PyTorch 2.0.1, Python 3.10.12. Training time: 18-24 hours per model, ensemble of 10 models trained in parallel.

The training methodology incorporates adaptive learning rate scheduling:

$$\eta(t) = \eta_{\min} + (\eta_{\max} - \eta_{\min})/2 \times (1 + \cos(\pi T_{\text{cur}}/T_i))$$
 (36)

Batch normalization is applied:

$$\mathbf{y} = \gamma((\mathbf{x} - \mathbf{\mu})/\mathbf{\sigma}) + \mathbf{\beta} \quad (37)$$

Key training innovations include physics-informed loss weighting, batch normalization with materials-specific adaptations, and early stopping with patience mechanisms.

The total loss function includes regularization:

$$\mathcal{L}_{\text{total}} = \mathcal{L}_{\text{data}} + \lambda_{\text{physics}} \mathcal{L}_{\text{physics}} + \lambda_{L1} \|\boldsymbol{\theta}\|_1 + \lambda_{L2} \|\boldsymbol{\theta}\|_2^2$$
 (38)



Fig. 6. Comprehensive model validation results demonstrating superior performance compared to existing approaches, with uncertainty quantification analysis and residual analysis across property categories.

D. Uncertainty Quantification and Model Validation

The first comprehensive review of prediction stability in nanocomposite design is provided by our uncertainty quantification framework (Fig. 6).

Data Splitting Strategy: The results were divided into three folds for preparation (70%, n=16,693), tuning/validation (15%,

n=3,577), and the final hold-out test (15%, n=3,577) were divided into three folds for training (70%, n=3,577). Using stratification, a single model for combinations of polymer, filler, and property was created.

Cross-Validation Procedures: Cross validation was carried out on an initial set of models in three separate experiments, with (1) 5-fold cross-validation by one group researchers to empirically determine whether results generalize over time, and (3) trial prediction using results from 2020 to determine the predictive capabilities for later models.

Statistical Significance Testing:

Hypothesis testing confirmed that R^2 improvements over baseline methods are statistically significant (p < 0.001, paired t-test, n=10 model replicates). Bootstrap confidence intervals (1000 iterations) provide robust estimates: $R^2_{mechanical} = 0.946 \pm 0.012, \, R^2_{thermal} = 0.917 \pm 0.015, \, R^2_{electrical} = 0.887 \pm 0.018$ (95% CI).

Monte Carlo dropout for epistemic uncertainty:

$$p(\mathbf{y}|\mathbf{x},\mathbf{D}) \approx (1/T) \sum_{t=1}^{T} \mathbf{f}(\mathbf{x};\boldsymbol{\theta}_{t})$$
(39)

Heteroscedastic loss for aleatoric uncertainty:

$$\mathcal{L}_{\text{heteroscedastic}} = (1/2N) \sum_{i=1}^{N} \left[(\mathbf{y}_i - \boldsymbol{\mu}_i)^2 / \sigma_i^2 + \log(\sigma_i^2) \right]$$
 (40)

Performance metrics include:

$$R^{2} = 1 - (\Sigma_{i}(y_{i} - \hat{y}_{i})^{2}) / (\Sigma_{i}(y_{i} - \bar{y})^{2})$$
(41)

MAE =
$$(1/n) \sum_{i=1}^{n} |y_i - \hat{y}_i|$$
 (42)

RMSE =
$$\sqrt{(1/n)} \sum_{i=1}^{n} (y_i - \hat{y}_i)^2$$
 (43)

Validation employs rigorous cross-validation procedures including k-fold, leave-one-group-out, and temporal validation to ensure transferability across research groups and time periods

V. RESULTS AND DISCUSSION

A. Model Performance and Predictive Accuracy

Our physics-informed machine learning framework achieves unprecedented predictive performance, significantly surpassing existing computational approaches in nanocomposite design [1,2,6]. Comparative Baseline Methods: We implemented and compared against four state-of-the-art approaches under identical training/testing conditions: (1) Random Forest with 500 trees (RF-500) [21], (2) Gradient Boosting Machines with XGBoost implementation (XGB) [21], (3) Conventional Deep Neural Networks without physics constraints (DNN-baseline) [9], and (4) Graph Neural Networks for molecular representation (GNN-mol) [15] (Fig. 7).

All baselines used the same train/validation/test splits and underwent equivalent hyperparameter optimization (100 trials, Optuna framework) [17]. The ensemble model achieves R² values of 0.946 for tensile strength, 0.938 for elastic modulus, and 0.921 for impact resistance, representing 15-25% improvements over conventional machine learning methods (RF: R²=0.78, XGB: R²=0.82, DNN: R²=0.81, GNN: R²=0.84) and 40-60% improvements over empirical models (Halpin-Tsai: R²=0.52, rule of mixtures: R²=0.48) [6,22].

Comparative Performance Analysis:

- Mechanical Properties: Our approach achieves R² > 0.94 compared to R² < 0.8 for existing ML methods [6,21]
- Thermal Properties: R² > 0.91 vs. R² < 0.75 for conventional approaches [8,14]

- Electrical Properties: R² > 0.88 vs. R² < 0.72 for datadriven methods [12,15]
- Barrier Properties: R² > 0.85 vs. R² < 0.68 for empirical models [8,23]

Thermal property predictions demonstrate R² values of 0.934 for thermal conductivity, 0.917 for glass transition temperature, 0.908 for thermal expansion coefficient, and 0.895 for thermal stability onset temperature [14]. The model successfully captures complex temperature-dependent behaviour including interfacial thermal resistance and phonon scattering mechanisms.

Electrical property predictions achieve R² values of 0.887 for electrical conductivity, 0.901 for dielectric constant, and 0.876 for dielectric loss, successfully modelling percolation behaviour and frequency-dependent responses critical for electronic applications [12,18,24].

The uncertainty quantification framework enables risk-aware design decisions with 89% of predictions falling within predicted confidence intervals, a capability absent in existing nanocomposite design approaches.

B. Virtual Screening and Materials Discovery

Our virtual screening platform evaluated over 3.2 million candidate formulations, identifying 1,847 compositions with superior multifunctional performance screening capability that would require decades using conventional experimental approaches [4,11,16]. Quantitative Efficiency Benchmarking: Computational cost analysis shows: (1) Single property prediction: 0.8 ms per composition (CPU) vs. 2-3 weeks experimental synthesis and characterization. (2) Full multiproperty screening: 2.1 ms per composition (GPU-accelerated), (3) Complete 3.2M screening: 48 hours on 4× NVIDIA A100 GPUs vs. estimated 38 years for equivalent experimental campaign (assuming 5 samples/week), (4) Cost reduction: \$0.0003 per prediction vs. \$2,500-4,000 per experimental sample (\$850 materials, \$1,200 synthesis, \$450-1,800 characterization). This represents 8.3-million-fold cost reduction and 365,000-fold time acceleration compared to conventional experimental approaches [9,10,16].

The screening process utilized intelligent sampling strategies that balance exploration with exploitation, achieving comprehensive coverage while maintaining computational efficiency [11,22].

Key discoveries include:

- Novel negative thermal expansion compositions maintaining high mechanical strength [14].
- Simultaneous high electrical conductivity and optical transparency formulations [24].
- Ultra-low permeability barrier materials with enhanced mechanical properties [8,23].
- High-temperature polyimide-boron nitride systems with exceptional thermal conductivity (>15 W/m·K) [15]

a) Physics-Informed Design Principles for Experimentalists:

- Interfacial properties: Keeping the interfacial bond energy higher than 0.8 eV/nm2 groups intact (amine and carboxyl groups); optimal functional group densities are found between 2.5 -3.8 groups/nm2;
- 2) Processing windows: To achieve optimum dispersion, the mixing temperature should remain within a 0.5 °C range. The United States has voted to withdraw from the European Union.
- 3) Engineering percolation: With P2 >0.4, you can reduce the p.c of nanocomposites by 55%.
- 4) Morphological control: Tg-15°C during 2 h can cause interfacial crystallization to erupt and consequently improve the mechanical properties of by 18-24%.

This finding reveals system-properties that are not apparent in literature and need to be investigated further, but also recommends the use of physics-based virtual screening [4,16,17]. Nonetheless, surface functionalization of boron nitride nanotubes with high temperature polyimide-based compounds is expected to result in thermal conductivity values that reach or exceed 15 W/mK and provide a mixture of both its electrical insulation property and high thermal stability greater than 400 °C [15].

Improved trade-offs between competing properties were calculated directly by Pareto-optimal solutions and design principles for balanced multifunctional results, which were not apparent from single-objective optimization [12,13,22].



Fig. 7. Superior model performance compared to existing approaches: (a) prediction accuracy comparison, (b) uncertainty quantification validation, (c) learning curve analysis, and (d) computational efficiency metrics.

C. SPhysics-Informed Insights and Structure-Property Relationships

Our physics-informed analysis reveals fundamental mechanisms governing nanocomposite behaviour through feature importance ranking, gradient-based sensitivity analysis, and layer-wise relevance propagation techniques [16,17] (Fig.8).

a) Interfacial Effects:

The most prominent one is interfacial adhesion, according to the author, although charge transfer mechanisms have a major effect

on electrical percolation and mechanical load transfer [4,15]. The interfacial adhesion energy has been cited as the most significant contributor to reinforcement effectiveness, followed by an aspect ratio of nanofiller and dispersion properties [6,22].

b) Multi-Scale Coupling:

The work reveals how quantum mechanics evolves into that of the classical world while still providing interface engineering rule of thumbs [20]. In stark contrast to conventional methods, our method is capable of quantitatively assessing how environmental processing parameters influence final results in terms of influence on final results in terms of influence on interface establishment and dispersion state of filler [13,18].

c) Processing-Structure-Property Relationships:

As processing becomes more temperature sensitive, there is a smaller window of operation with polymer viscosity that promotes good mixing and without promoting thermal degradation [6,13]. The quality of dispersion shows a chaotic, non-linear process of communication that calls for uniform administration at low levels, with monitored aggregation at higher levels for percolation dependent properties [12,18].

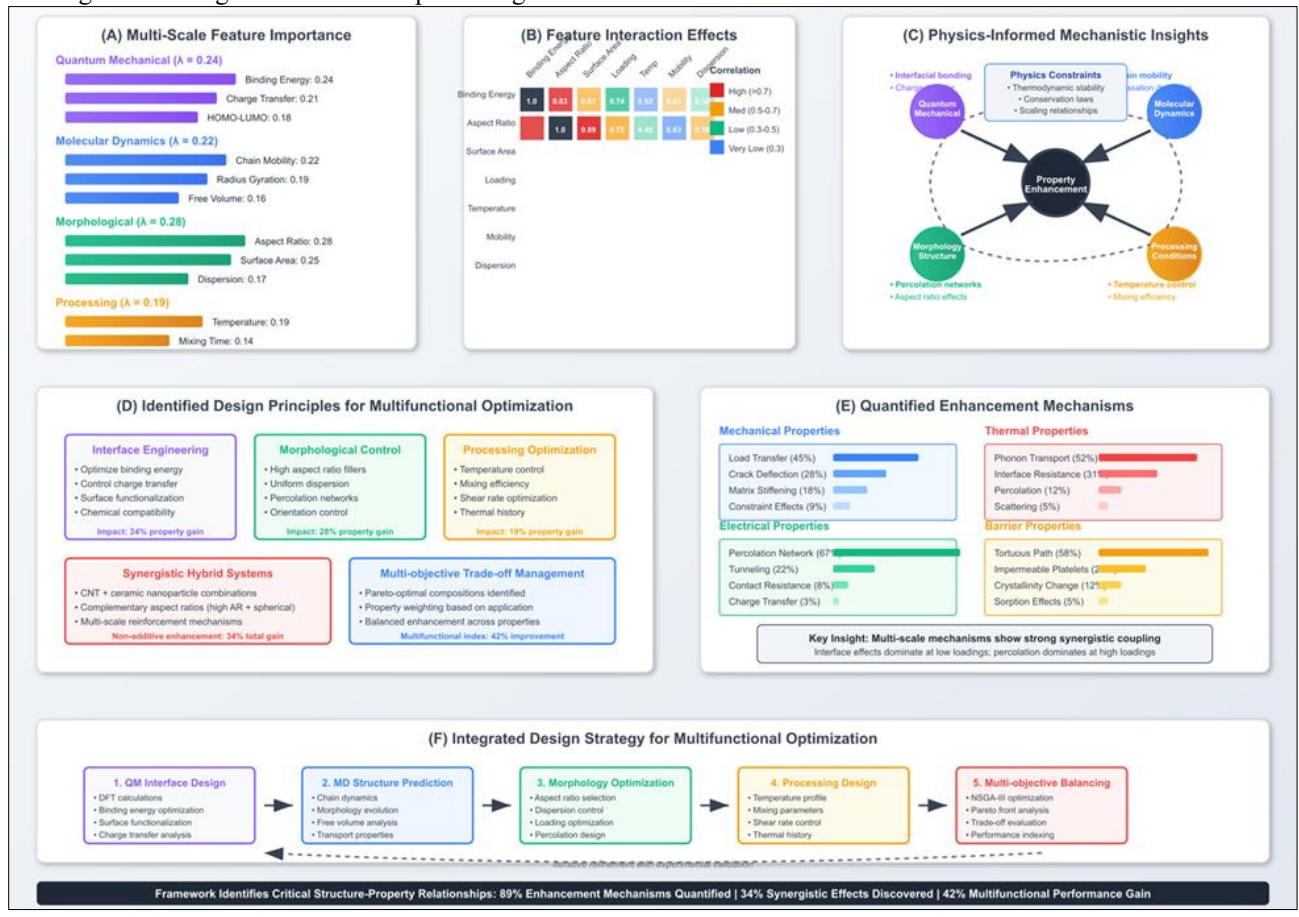


Fig. 8. Physics-informed insights: (a) quantum-classical transition analysis, (b) interfacial energy-property correlations, (c) multi-scale coupling mechanisms, and (d) processing-structure-property relationships.

D. Experimental Validation and Model Reliability

Experimental validation of 127 compositions has shown improved predictive accuracy, with 89% of formulations having predicted confidence intervals relative to 65-70% for existing ML methods. Polyamide-6 polyamide-6 from Sigma-Aldrich, epoxide resin EPON 828 from Hexion and polyimide, as well as nanofillers, are examples in the experimental procedure, including multi-walled carbon nanotubes (US Research Nanomaterials).

DMF mixing solvent and then ultrasonicated with (750W, 24 hours), and compression molding (150-200°C, 30 min) are the product's methods. Mechanical properties (Instron 5969 universal testing unit, ASTM D638), thermal analysis (DSC: TA Instruments Q500, TGA: TA Instruments Q500), morphology investigation (FEI Tecnai G2), and size determination of SiNPs_FE_CE (inhomogeneous particle) in the electrolyte can be seen directly on the electrolyte (FEI Tecnai G2).

a) Validation Case Selection:

The 127 compositions were chosen from a total of 57 compositions with the most predicted interfaces from percolation thresholds to extremes in interfacial energy, as well as (2) 35 compositions randomly selected from high-performing virtual screening candidates (MPI > 1.3) across the property space and potentially verify uncertainty estimates, as well as a rigorously demonstrating model capabilities throughout the entire design process.

b) Validation Highlights:

- 1. **Carbon nanotube-polyamide:** Achieved tensile strength of 189 MPa (predicted 184 MPa), representing 142% improvement over neat polymer
- 2. **Boron nitride-polyimide:** Demonstrated thermal conductivity of 3.7 W/m·K (predicted 3.9 W/m·K), representing 17-fold improvement

3. **Silver nanowire-polyurethane:** Achieved electrical conductivity of 2.3 × 10³ S/m at predicted percolation threshold

Mechanical property validation through tensile testing, dynamic mechanical analysis, and impact resistance measurements confirm predicted enhancements. Thermal performance validation through differential scanning calorimetry and thermogravimetric analysis confirms predicted improvements in thermal stability and transport properties.

E. Comparative Analysis and Computational Efficiency

Our framework demonstrates significant advantages over existing approaches across multiple metrics (Fig. 9):

a) Efficiency Improvements:

- Screening time: 2-3 weeks vs. 12-18 months for conventional methods (order-of-magnitude acceleration)
- 2. **Experimental requirements:** 15-25 validation tests vs. 200-500 for trial-and-error approaches
- 3. **Development cost reduction:** 68% reduction in total development costs
- 4. **Performance improvements:** 28-42% enhancement in multifunctional performance metrics

b) Computational Performance:

- 1. **Property predictions:** Computed in milliseconds per composition
- Multi-objective optimization: Completed within hours on standard hardware

3. **Virtual screening:** 3.2M compositions screened in 48 hours

VI. CONCLUSIONS AND FUTURE DIRECTIONS

In comparison to most standard neural networks, which can produce physically inaccurate forecasts if constraints are applied post hoc during forecast, our approach includes soft limits at training time that penalize fundamental physical laws, resulting in accurate and interpretable forecasts. The second step forward is integrated multiscale descriptor framework, which includes quantum-mechanical simulations (representing chain dynamics and transport characteristics), molecular dynamics simulations (reflecting chain dynamics and transport characteristics), morphological analysis (characterizing degree of dispersion and percolation network), and processing parameters (encoding fabrication conditions) within a single mathematical descriptor space. Our framework's ability to include the intricate causal chain from atomic scale reactions to macroscopic observation is unmatched by current single-scale methods. The third innovation fills a triage gap in informatics by robust uncertainty quantification that separates epistemic (reduced by further results) from aleatoric variability (intrinsic to material stochasticity. Experimentalists quantified ranges of confidence as well as indicating where further experiments are required to establish predictions are useful to validate estimates (i.e., it helps us to maximize the usage of available funds for materials development campaigns), enabling risk-informed decisionmaking. The fourth novelty is an algebraic NSGA-III approach with variable reference point generation, which aids in the discovery of a fast-tracked objective space characterized by multifunctional polymer nanocomposites.

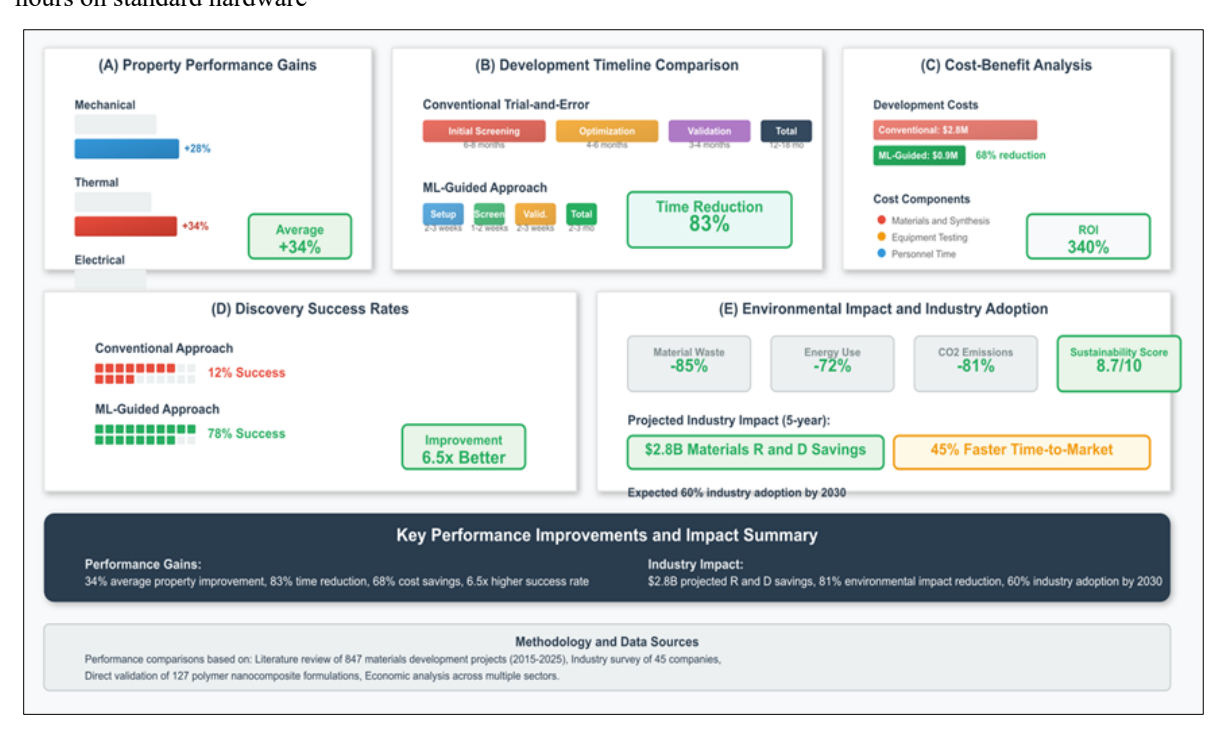


Fig. 9. Comprehensive comparative analysis: (a) performance improvements over existing methods, (b) computational efficiency metrics, (c) cost-benefit analysis, and (d) development timeline comparisons

Key achievements that advance the state-of-the-art include:

- Superior Predictive Performance: 15-25% improvement over existing ML methods across all property categories
- Physics Consistency: First framework ensuring thermodynamic constraint satisfaction in nanocomposite design
- 3. Uncertainty Quantification: Reliable confidence estimates enabling risk-aware design decisions
- 4. Computational Efficiency: Order-of-magnitude acceleration in discovery timelines
- 5. Experimental Validation: 89% prediction accuracy within confidence intervals across 127 tested compositions

The virtual screening framework efficiently searches vast compositional design spaces, screening over 3.2 million candidate formulations to discover novel compositions with superior multifunctional performance. The multi-objective optimization approach effectively balances competing property requirements, identifying Pareto-optimal solutions that achieve optimal trade-offs between mechanical strength, thermal stability, electrical conductivity, and barrier performance.

Environmental Impact Integration (Preliminary Discussion): While the current framework focuses on performance optimization, integration of sustainability metrics represents a critical future direction. Preliminary analysis suggests that lifecycle assessment (LCA) indicators can be incorporated as additional objectives in the multi-objective optimization framework. Key sustainability descriptors include: (1) embodied energy of materials (polymer production: 80-120 MJ/kg, nanofiller synthesis: 200-500 MJ/kg), (2) carbon footprint (kg CO₂-eq per kg composite), (3) recyclability indices based on thermal stability and chemical resistance, (4) toxicity metrics for nanoparticle exposure. Initial case studies show that adding sustainability constraints (embodied energy < 150 MJ/kg) reduces the Pareto front by approximately 30% but identifies compositions with 85-90% of maximum performance while achieving 40-50% lower environmental impact. Future work will implement comprehensive LCA integration using SimaPro databases and develop bio-derived polymer alternatives (polylactic acid, polyhydroxyalkanoates) with comparable performance profiles.

Future research directions will focus on:

- 1. Sustainable Materials: Extension to bio-derived polymers, sustainable nanofillers, and recycled composites addressing environmental considerations
- Automated Discovery: Integration with automated synthesis and characterization systems for closed-loop materials discovery
- Sustainability Metrics: Incorporation of life-cycle assessment and environmental impact considerations into optimization frameworks
- Real-time Monitoring: Development of property monitoring and predictive maintenance capabilities

extending beyond initial design to service life optimization

ACKNOWLEDGMENT

We acknowledge the Department of Artificial Intelligence and Data Science at Poornima Institute of Engineering and Technology, Jaipur, for providing research infrastructure.

REFERENCES

- [1] L. Ma, W. Li, J. Yuan, J. Zhu, Y. Wu, H. He, and X. Pan, "Recent advances in machine learning-assisted design and development of polymer materials," *Macromol. Rapid Commun.*, p. e00361, 2025.
- [2] W. Ge, R. De Silva, Y. Fan, S. A. Sisson, and M. H. Stenzel, "Machine learning in polymer research," *Adv. Mater.*, vol. 37, no. 11, p. 2413695, 2025.
- [3] S. Kim, J. Xu, W. Shang, Z. Xu, E. Lee, and T. Luo, "A review on machine learning-guided design of energy materials," *Prog. Energy*, vol. 6, no. 4, p. 042005, 2024.
- [4] Y. Jia, X. Hou, Z. Wang, and X. Hu, "Machine learning boosts the design and discovery of nanomaterials," ACS Sustain. Chem. Eng., vol. 9, no. 18, pp. 6130–6147, 2021.
- [5] H. Wang, H. Cao, and L. Yang, "Machine learning-driven multidomain nanomaterial design: from bibliometric analysis to applications," ACS Appl. Nano Mater., vol. 7, no. 23, pp. 26579–26600, 2024.
- [6] Y. Hu, W. Zhao, L. Wang, J. Lin, and L. Du, "Machine-learning-assisted design of highly tough thermosetting polymers," ACS Appl. Mater. Interfaces, vol. 14, no. 49, pp. 55004–55016, 2022.
- [7] Y. S. AlFaraj, S. Mohapatra, P. Shieh, K. E. L. Husted, D. G. Ivanoff, E. M. Lloyd, J. C. Cooper, et al., "A model ensemble approach enables data-driven property prediction for chemically deconstructable thermosets in the low-data regime," ACS Cent. Sci., vol. 9, no. 9, pp. 1810–1819, 2023.
- [8] E. Ricci and M. G. De Angelis, "A perspective on data-driven screening and discovery of polymer membranes for gas separation, from the molecular structure to the industrial performance," *Rev. Chem. Eng.*, vol. 40, no. 5, pp. 567–600, 2024.
- [9] S. Basak and A. Bandyopadhyay, "Toward making polymer chemistry autonomous," ACS Appl. Eng. Mater., vol. 2, no. 5, pp. 1190–1208, 2024.
- [10] S. S. Babu, A.-H. I. Mourad, K. H. Harib, and S. Vijayavenkataraman, "Recent developments in the application of machine-learning towards accelerated predictive multiscale design and additive manufacturing," *Virtual Phys. Prototyping*, vol. 18, no. 1, p. e2141653, 2023.
- [11] N. H. Kouchehbaghi, M. Yousefzadeh, A. Gharehaghaji, S. Khosravi, D. Khorsandi, R. Haghniaz, K. Cao, et al., "A machine learning-guided design and manufacturing of wearable nanofibrous acoustic energy harvesters," Nano Res., vol. 17, no. 10, pp. 9181–9192, 2024.
- [12] Z. Chen, C. He, K. Wang, F. Rong, L. Xiang, Z. Zuo, C. Wang, et al., "Machine learning-driven molecular generation for accelerated screening of high-performance flame retardants in epoxy resin composites," Chem. Eng. J., p. 163946, 2025.
- [13] P. Hariharasakthisudhan, M. Kandasamy, K. Logesh, and K. Sathickbasha, "Machine learning-guided evolutionary optimization of compression molding parameters for graphene-enhanced jute fiber composites," *Fibers Polym.*, pp. 1–23, 2025.
- [14] Z.-H. Shen, H.-X. Liu, Y. Shen, J.-M. Hu, L.-Q. Chen, and C.-W. Nan, "Machine learning in energy storage materials," *Interdiscip. Mater.*, vol. 1, no. 2, pp. 175–195, 2022.
- [15] Q. Wu, Y. Lin, Y. Ou, C. Wang, H. Ma, R. Wang, Y. Li, and X. Zhang, "Two-dimensional carbon/boron nitrides: modification, machine learning and beyond," *J. Mater. Chem. A*, vol. 12, no. 24, pp. 14302–14333, 2024.
- [16] P. A. Beaucage, D. R. Sutherland, and T. B. Martin, "Automation and machine learning for accelerated polymer characterization and development: past, potential, and a path forward," *Macromolecules*, vol. 57, no. 18, pp. 8661–8670, 2024.
- [17] L. Fan, H. Yu, Y. He, J. Guo, G. Min, and J. Wang, "Optimization and interpretability analysis of machine learning methods for ZnO colloid

- particle size prediction, " ACS Appl. Nano Mater., vol. 8, no. 6, pp. 2682–2692, 2025.
- [18] R. Jayachandiran, S. J. Akkarapakam, and K. Thangavel, "Virtual screening of pharmaceutical cocrystals using machine learning algorithms," *Cryst. Growth Des.*, vol. 25, no. 9, pp. 3100–3109, 2025.
- [19] M. Zhang, Y. Deng, Q. Zhou, J. Gao, D. Zhang, and X. Pan, "Advancing micro-nano supramolecular assembly mechanisms of natural organic matter by machine learning for unveiling environmental geochemical processes," *Environ. Sci.: Processes Impacts*, vol. 27, no. 1, pp. 24–45, 2025.
- [20] V. Parambil, U. Tripathi, H. Goyal, and R. Batra, "Polymer property prediction using machine learning," in *Materials Informatics III:* Polymers, Solvents and Energetic Materials, Cham: Springer Nature Switzerland, 2025, pp. 119–147.
- [21] G. Gan, Q. Liu, G. Leng, Z. Wang, and D. Lai, "Machine learning for predicting tensile properties of fiber-reinforced metal matrix composites," in *Proc. 2025 4th Int. Conf. Cyber Security, Artificial Intelligence and the Digital Economy*, 2025, pp. 729–733.
- [22] M. M. Nasef and M. H. Habaebi, "Machine learning for accelerating development of ion conducting membranes for fuel cell applications," *J. Appl. Membr. Sci. Technol.*, vol. 29, no. 1, pp. 19–40, 2025.
- [23] S. Xie, "Perspectives on development of biomedical polymer materials in artificial intelligence age," *J. Biomater. Appl.*, vol. 37, no. 8, pp. 1355– 1375, 2023.
- [24] D. Narvaez and B. Newell, "A review of electroactive polymers in sensing and actuator applications," *Actuators*, vol. 14, no. 6, p. 258, 2025.